การตรวจวัดปรอทในระดับต่ำโดยใช้อนุภาคทองคำดัดแปรระดับนาโนเมตร

นางสาววิภาวี เลี้ยงรักษา

DETERMINATION OF MERCURY IN TRACE LEVEL USING MODIFIED GOLD
NANOPARTICLES

Miss Viphavee Liangraksa

A Thesis Submitted in Partial Fulfillment of the Requirements

for the Degree of Master of Science Program in Chemistry

Department of Chemistry

Faculty of Science

Chulalongkorn University

Academic Year 2013

Thesis Title   DETERMINATION OF MERCURY IN TRACE LEVEL
                     USING MODIFIED GOLD NANOPARTICLES
By   Miss Viphavee Liangraksa
Field of Study   Chemistry
Thesis Advisor   Assistant Professor Fuangfa Unob, Ph.D.
Thesis Co-Advisor   Luxsana Dubas, Ph.D.

Accepted by the Faculty of Science, Chulalongkorn University in Partial Fulfillment of the Requirements for the Master's Degree

⋯⋯⋯⋯⋯⋯⋯⋯⋯⋯Dean of the Faculty of Science

(Professor Supot Hannongbua, Dr.rer.nat.)

THESIS COMMITTEE

⋯⋯⋯⋯⋯⋯⋯⋯⋯⋯Chairman

(Associate Professor Vudhichai Parasuk, Ph.D.)

⋯⋯⋯⋯⋯⋯⋯⋯⋯⋯Thesis Advisor

(Assistant Professor Fuangfa Unob, Ph.D.)

⋯⋯⋯⋯⋯⋯⋯⋯⋯⋯Thesis Co-Advisor

(Luxsana Dubas, Ph.D.)

⋯⋯⋯⋯⋯⋯⋯⋯⋯⋯Examiner

(Monpichar Srisa-art, Ph.D.)

⋯⋯⋯⋯⋯⋯⋯⋯⋯⋯External Examiner

(Sujitra Srisung, Ph.D.)

วิภาวี เลี้ยงรักษา : การตรวจวัดปรอทในระดับต่ำโดยใช้อนุภาคทองคำดัดแปรระดับนาโนเมตร. (DETERMINATION OF MERCURY IN TRACE LEVEL USING MODIFIED GOLD NANOPARTICLES) อ.ที่ปรึกษาวิทยานิพนธ์หลัก: ผศ. ดร.เฟื่องฟ้า อุ่นอบ, อ.ที่ปรึกษาวิทยานิพนธ์ร่วม: อ. ดร.ลักษณา ดูบาส, 44 หน้า.

ในงานวิจัยนี้ได้พัฒนาวิธีการตรวจวัดไอออนปรอท(II) ในระดับต่ำที่มีความว่องไวสูงสองวิธี ได้แก่ การตรวจวัดโดยใช้สารละลายอนุภาคทองคำระดับนาโนเมตรดัดแปรด้วยแอลซิสเตอีน และการตรวจวัดโดยใช้ซิลิกาที่เคลือบด้วยอนุภาคทองคำระดับนาโนเมตรที่ดัดแปรด้วยแอลซิสเตอีน ในระบบสารละลาย อนุภาคทองคำดัดแปรระดับนาโนเมตรถูกเหนี่ยวนำให้รวมตัวกันเป็นกลุ่มโดยไอออนปรอท(II) ส่งผลให้เกิดการเปลี่ยนแปลงสีของสารละลายจากสีแดงเป็นสีน้ำเงิน ตรวจวัดผลที่เกิดขึ้นด้วยเครื่องยูวีวิสสิเบิลสเปคโตรโฟโตมิเตอร์ที่ความยาวคลื่น 670 และ 520 นาโนเมตร ทำการหาสภาวะที่ดีที่สุดของตัวแปรที่ส่งผลต่อการวิเคราะห์ปริมาณไอออนปรอท(II) ได้แก่ เวลาการดัดแปรผิว ความเข้มข้นของโซเดียมคลอไรด์ เวลาการตรวจวิเคราะห์ ปริมาตรตัวอย่าง และผลของไอออนร่วม ช่วงความเป็นเส้นตรงของวิธีการนี้ คือ 5-40 ไมโครกรัมต่อลิตร และขีดจำกัดต่ำสุดของการตรวจวัด คือ 4.5 ไมโครกรัมต่อลิตร ส่วนในระบบของแข็ง ทำการเคลือบผิวซิลิกาด้วยอนุภาคทองคำระดับนาโนเมตร และดัดแปรผิวอนุภาคด้วยแอลซิสเตอีน เพื่อใช้เป็นเฟสสำหรับสกัดและตรวจวัดไอออนปรอท(II) และเพื่อเพิ่มความจำเพาะเจาะจงในการตรวจวัดปรอทได้ทำการรีดิวซ์ไอออนปรอทบนเฟสของแข็งด้วยสารละลายทิน(II) คลอไรด์ โดยสีของเฟสจะเปลี่ยนจากสีชมพูเป็นสีม่วงและสีน้ำเงินตามลำดับ ตามความเข้มข้นของไอออนปรอท(II) ทำการศึกษาตัวแปรที่ส่งผลต่อการวิเคราะห์ปริมาณไอออนปรอท(II) ได้แก่ ความเข้มข้นอนุภาคทองคำระดับนาโนเมตร เวลาการเคลือบอนุภาคทองคำระดับนาโนเมตรบนซิลิกา ความเข้มข้นของสารละลายแอลซิสเตอีน เวลาการสกัด ความเข้มข้นของสารละลายทิน(II) คลอไรด์ และผลของไอออนร่วม ซึ่งวิธีนี้สามารถตรวจวัดไอออนปรอท(II) ด้วยตาเปล่าในช่วง 2-100 ไมโครกรัมต่อลิตร และได้ประยุกต์ใช้วิธีการเหล่านี้ในการวิเคราะห์ปรอทในน้ำดื่มและน้ำประปา

ภาควิชา เคมี	ลายมือชื่อนิสิต ....
สาขาวิชา เคมี	ลายมือชื่อ อ.ที่ปรึกษาวิทยานิพนธ์หลัก ....
ปีการศึกษา 2556	ลายมือชื่อ อ.ที่ปรึกษาวิทยานิพนธ์ร่วม ....

VIPHAVEE LIANGRAKSA: DETERMINATION OF MERCURY IN TRACE LEVEL USING MODIFIED GOLD NANOPARTICLES. ADVISOR: ASST. PROF. FUANGFA UNOB, Ph.D., CO-ADVISOR: LUXSANA DUBAS, Ph.D., 44 pp.

Highly sensitive methods for trace level mercury(II) ions detection was developed. Two methods are proposed in this research; the use of L-cysteine modified gold nanoparticles (cys-AuNPs) solution and the use of L-cysteine modified gold nanoparticles supported silica (cys-AuNPs-Si). In the solution system, the aggregation of cys-AuNPs was induced by mercury(II) ions resulting in the change of solution color from red to blue. The phenomenon was investigated by UV-Visible spectrophotometer at 670 and 520 nm. The effect of parameters affecting mercury(II) determination including modification time, NaCl concentration, detection time, sample volume and co-existing ions were investigated. The linear range of this method was obtained in a range of 5 to 40 µg/L and detection limit was as low as 4.5 µg/L. In the solid system, gold nanoparticles were coated on silica and further modified with L-cysteine (cys-AuNPs-Si) for mercury(II) ions extraction and sensing. To improve the selectivity of mercury(II) detection, the extracted mercury(II) ions on cys-AuNPs-Si phase were reduced with tin(II) chloride. The color of the solid phase changed from pink to purple and blue depending on mercury(II) concentration. The effect of parameters affecting mercury(II) determination including AuNPs concentration, coating time, L-cysteine concentration, extraction time, tin(II) chloride concentration, co-existing ions were studied. The proposed method could detect mercury by naked eyes in a range of 2 to 100 µg/L. Finally, these methods were applied to the analysis of drinking and tap water.

Department:	Chemistry	Student's Signature	....
Field of Study:	Chemistry	Advisor's Signature	....
Academic Year:	2013	Co-Advisor's Signature	....

ACKNOWLEDGEMENTS

CONTENTS

LIST OF TABLES

Table   Page

LIST OF FIGURES

Figure **Page**

LIST OF ABBREVIATIONS

M	Molar
μM	Micromolar
nm	Nanometer
mg/L	Milligram per liter
μg/L	Microgram per liter
mL	Milliliter
μL	Microliter
$^{\circ}$C	Degree Celsius
CTAB	Hexadecyltrimethylammonium bromide
Cys	L-cysteine
AuNPs	Gold nanoparticles

CHAPTER I

INTRODUCTION

1.1 Statement of the problem

Nowadays, human activities and natural processes cause contamination of heavy metals in environments such as in soil, air or water. The contamination causes several pollutions and damages our health. Among the toxic metals, mercury is one of the most hazardous heavy metals. Mercury can damage the nervous system, brain, kidney and many other organs [1-3]. Therefore, monitoring of mercury is necessary. The Pollution Control Department (Thailand), mercury level in surface water and waste water should not exceed 2 and 5 µg/L, respectively. In addition, by the World Health Organization (WHO), mercury levels should not higher than 2 µg/L in drinking water [4].

Currently, there are many techniques for mercury determination such as electrochemical methods [5, 6], cold vapor atomic absorption spectrometry (CV-AAS) [7], cold vapor atomic emission spectrometry (CV-AES) [8], atomic fluorescence spectrometry (AFS) [9, 10], inductively coupled plasma atomic emission spectrometry (ICP-AES) [11-13], inductively coupled plasma mass spectrometry (ICP-MS) [14, 15]. Although these techniques yield high accuracy, precision and sensitivity, the expert operators and expensive devices are required.

Analysis of mercury using gold nanoparticles (AuNPs) is a choice to reduce above restrictions. There have been used as the colorimetric sensors using localized surface plasmon resonance (LSPR) properties. This phenomenon is associated with the color of gold nanoparticles solution and absorption spectral [16]. LSPR properties of gold nanoparticle depend on many factors including its shape and size as well as dielectric surrounding particles and inter-particle distance. Moreover, the surface of AuNPs could be easily modified with specific functional groups Therefore, AuNPs have been applied to monitor several analytes including Hg(II) ion[17-20].

In this study, a sensitive method to determine Hg(II) ions in the trace level was improved using modified gold nanoparticles with L-cysteine. Based on AuNPs aggregation, the solution color change was observed by necked eyes and UV-Visible spectrophotometer.

1.2 Objectives of the thesis

1. To develop a method to analyze trace Hg(II) ions.

2. To apply the developed method to analyze Hg(II) ions in real water samples.

1.3 Scope of the thesis

In the first section, tri-sodium citrate di-hydrate ($Na_3C_6H_5O_7 \cdot 2H_2O$) as a reducing agent, and stabilizer was employed in a gold nanoparticle synthesis process. Then, a selective ligand, L-cysteine, was modified on AuNPs surface as a Hg(II) ions sensing agent. Various parameters affecting the LSPR properties of AuNPs such as modification time, NaCl concentration, detection time, sample volume and co-existing ions were investigated. Finally, the proposed method was validated and applied for the determination of Hg(II) in real water samples.

In the second section, tri-sodium citrate di-hydrate ($Na_3C_6H_5O_7 \cdot 2H_2O$), a reducing agent, and hexadecyl trimethyl ammonium bromide (CTAB), a stabilizer, were employed in gold nanoparticles synthesis process. Then, the CTAB-AuNPs was coated on silica surface. Afterward, a selective ligand as L-cysteine was modified on AuNPs surface as a Hg(II) ions sensing agent. The solid phase was used to extract Hg(II) ions in the solution. Then, the extracted Hg(II) ions was reduced to Hg(0). The various parameters affecting the SPR properties of AuNPs such as AuNPs concentration, coating time, L-cysteine concentration, extraction time, reducing agent concentration and co-existing ions were investigated. Finally, the proposed method was also validated and applied for real water samples.

1.4 The benefit of this research

A sensitivity and simple analysis method to determine trace Hg(II) ions in water samples using modified gold nanoparticles was obtained.

CHAPTER II

THEORY AND LITERATURE REVIEW

2.1 Measurement of mercury

Due to Hg(II) hazard to all living things and environment, it is necessary to monitor the amount of Hg(II) ions in environmental samples and consumer products. There are many methods applied for determination of mercury including spectrophotometry. However, the major problem in mercury measurement is the low sensitivity of the instrument. Therefore, pre-concentration of sample is often required to improve the sensitivity of the method. Several methods have been proposed for Hg(II) ions detection in different samples as follows.

Bansal *et al.* [21] proposed a method to determine total mercury in bauxite and bauxite residue. The sample was prepared by acid digestion for changing all mercury species to their soluble ionic form. Then, all ions of mercury were determined by cold vapor atomic absorption spectrometry (CV-AAS). The limit of detection of the method was 0.023 µg/kg.

Lemos *et al.* [22] developed a highly sensitive method for determination of mercury in human saliva. Mercury(II) ions were pre-concentrated using solid phase extraction (SPE). A complexing agent 2-(2'-benzothiazolylazo)-p-cresol (BTAC) trapped Hg(II) ions in SPE column and the metal ions were eluted with 1.75 M HCl before being detected by CV-AAS. The limit of detection of the method was 0.011 µg/L.

Moreover, there were also methods that combined spectrometric and chromatographic techniques for mercury speciation. For example, Pietilä *et al.* [23] developed a highly sensitive method for determination of methyl mercury in natural water sample using gas chromatography (GC) coupled with inductively coupled plasma mass spectrometry (ICP-MS). The limit of detection of the method was 0.05 ng/L.

From previous work, there are many methods for detection of trace level Hg(II) ions in water samples and the sample preparation or pre-concentration was usually used before instrumental analysis. Although, these methods could improve the limit of Hg(II) ions detection, there are also some weak points, such as time-consumption and complicated instrument and process. Therefore, colorimetric and spectrophotometric methods are an attractive alternative for Hg(II) ions detection.

Hg(II) ions could be detected through specific ligand-analytes complex formation by following the change in their colors and intensities. Furthermore, nanoparticles such as gold nanoparticles, silver nanoparticles and quantum dots have been used for this purpose due to their optical properties and the ease in their surface modification with various types of ligand [24, 25]. In this case, some colorimetric sensors and spectrophotometric methods are reviewed as follows.

Hua Jin *et al*. [26] presented a simple method for Hg(II) ions determination in tap water by using gold nanorod (AuNRs) as a colorimetric sensor. The AuNRs were stabilized with hexadecyl trimethyl ammonium bromide (CTAB). In the presence of ascorbic acid (AA), the amalgamation process between Hg(0) and Au(0) was obtained. The detection limit of this method was 0.2 mg/L.

Maity *et al*.[27] developed a method for determination of Hg(II) ions in aqueous media by using gold nanoparticles (AuNPs) modified with dithiocarbamate derivative of calixarene. The change of AuNPs color was observed from red to violet in the presence of Hg(II) ions due to the aggregation of AuNPs. The detection limit of this method was 0.04 mg/L.

2.2 Gold nanoparticles

Gold nanoparticles (AuNPs) are colloidal that have particles size in the range of 1 to 100 nm. They have distinct properties when compared to Au(III) ions properties including physical and chemical properties. For example, the color of Au(III) ions solution is yellow but the color of AuNPs solution has red tone color depending on their size such as a dark red color of 8 nM AuNPs, a red color of 13 nM AuNPs, a pinkish red color of 32 nM AuNPs or a pink color of 55 nM AuNPs [28]. The change in color of AuNPs solution can be described by their surface plasmon resonance (SPR) properties.

The phenomenon of surface plasmon resonance (SPR) is an optical property of nanoparticles such as gold nanoparticles (AuNPs) and silver nanoparticles (AgNPs). This phenomenon is a result of free electron oscillation on the metal surface due to frequency matching between surface electrons and the incident light as shown in Figure 2.1 [16].
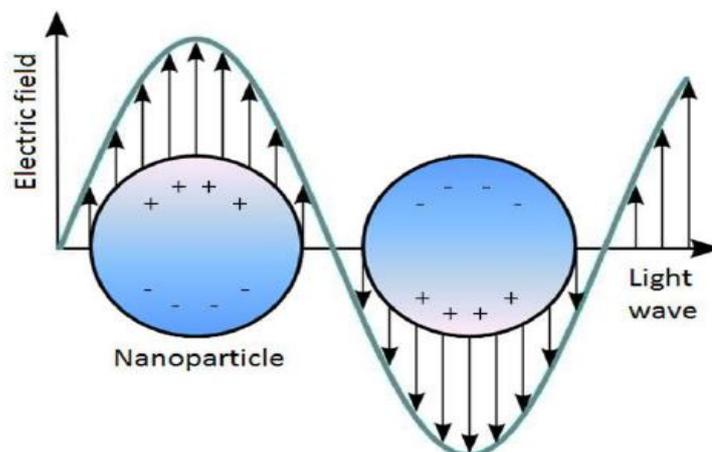
Figure 2.1 The electromagnetic field direction of nanoparticles [29].

Surface plasmon resonance (SPR) is called instead of the electromagnetic field of metal nanoparticles. SPR bands can be observed by following absorbance intensities and the maximum absorption wavelength (λ_{max}) of metal nanoparticles solution by UV-Visible spectrophotometer. The SRP band of various metal nanoparticles depends on the type, size and shape of metal nanoparticles, inter-particle distances of metal nanoparticles and dielectric constant of surrounding media [16]. For gold nanoparticles (AuNPs), the SPR band at 13 nm occurs in the range of visible light with λ_{max} at 520 nm resulting in a red color of solution. The spectra of AuNPs aggregation show the red shift of λ_{max} to longer wavelengths and the solution color changes from red to purple and blue, respectively. From above mentioned optical properties, gold nanoparticles have been used as sensors to determine several analytes such as biomolecules [30], biomedical compounds [31] and metal ions [32].

Furthermore, the reason of an extensive use of AuNPs is due to its unique properties and the ease of preparation. AuNPs solutions can be prepared by using reducing agents such as trisodium citrate [33, 34], cetyl trimethyl ammonium bromide (CTAB) [35-37], polymers [38], sodium borohydride and ascorbic acid [39] to reduce Au(III) ions to AuNPs. The commonly used method of AuNPs preparation is the reduction with tri-sodium citrate because sodium citrate can act both as a reducing agent and a stabilizer. The citrate anions are adsorbed on the surface of AuNPs to produce negatively charged surface that prevent the aggregation of AuNPs

resulting in stable colloidal AuNPs. The reaction in AuNPs preparation with citrate reduction is shown below [40].

$$2\,AuCl_3 + 3\,(^-OCCH_2)_2C(OH)CO^- \longrightarrow 2\,Au^o + 3\,(^-OCCH_2)_2C{=}O + 6\,Cl^- + 3\,H^+ + 3\,CO_2$$
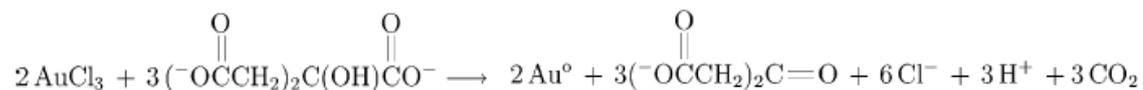
Moreover, the charges surrounding AuNPs could be adjusted to be negative or positive using a cationic or anionic surfactant as a stabilizer. For example, CTAB which is a cationic surfactant can be added to citrate capped AuNPs as a stabilizer. When CTAB molecules are adsorbed around citrate anions on AuNPs surface, CTAB bilayer would form on the AuNPs surface and prevent the aggregation of AuNPs. The bilayer of CTAB on AuNPs surface is proposed as shown in Figure 2.2.
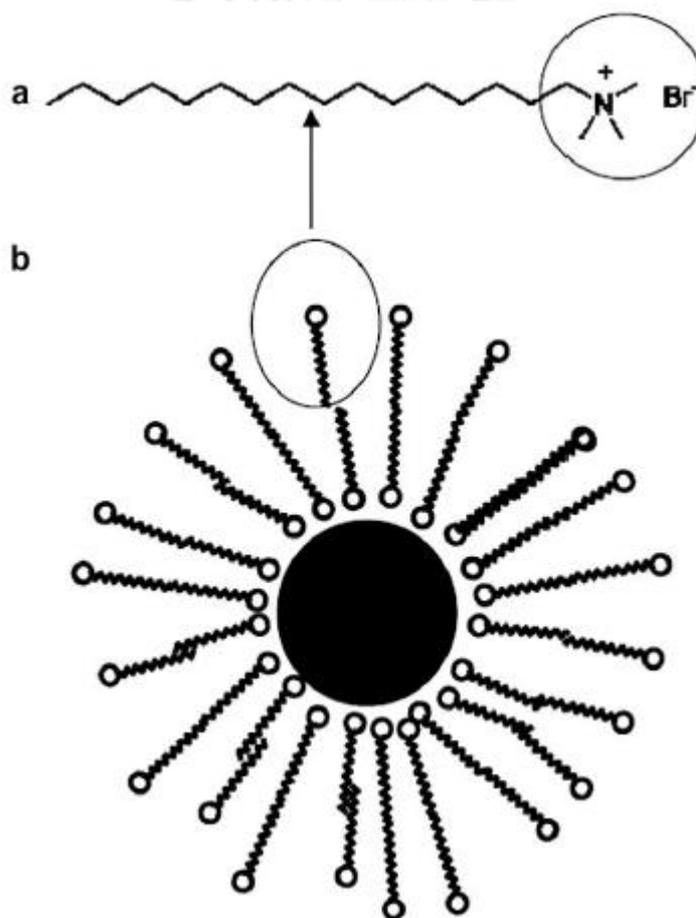
Figure 2.2 (a) Structure of CTAB and (b) CTAB bilayer on AuNPs surface [41]

2.3 Literature review

Gold nanoparticles (AuNPs) have been widely used in several applications in chemical analysis due to their optical properties. There are many researches that proposed the use of AuNPs in the determination of Hg(II) ions level. Based on the aggregation or disaggregation of AuNPs, the change of solution color and SPR band were observed by both necked eyes and UV-Visible spectrophotometer. The method selectivity could be improved by using selective ligands for Hg(II) ions to modify AuNPs as reported below.

Wu *et al.* [42] developed a highly sensitive method for determination of Hg(II) ions in water sample by using gold nanoparticles (AuNPs) modified with DNA. The Hg(II) ions could coordinate with thymine of DNA and induce DNA-AuNPs aggregation. The change of AuNPs solution color was observed from red to blue. The detection limit of this method was 12 μg/L.

Chansuvarn *et al.* [43] developed a selective and simple method for determination of Hg(II) ions in water by following the formation of gold nanoparticles and mercury amalgam. The solution of Au(III) was mixed with dithia-diaza ligand 2-[3-(2-amino-ethylsulfanyl)-propylsulfanyl]-ethylamine (AEPE) and Hg(II) ions solution. Afterward, this mixed solution was reduced with $NaBH_4$ for amalgamation process. In the presence of Hg(II), the color of solution changed from red to blue. The detection limit of this method was 7 μg/L.

Ding *et al.* [44] proposed the use of gold nanoparticles that were prepared by the reduction of Au(III) ions with poly(diallyldimethylammonium) chloride (PDDA) and PDDA acted both as a reducing agent and a stabilizer. The PDDA-AuNPs were further modified with L-cysteine that induced the nanoparticles aggregation. In the presence of Hg(II) ions, Hg(II) ions would form complexes with L-cysteine resulting in the release of L-cysteine from PDDA-AuNPs. Therefore, the sensing mechanism was to disaggregate the nanoparticles and AuNPs solution color in presence of Hg(II) ions changed from blue to red. The linear range of determination was 10 to 2000 μg/L (r^2 = 0.996). The detection limit of this method was 5 μg/L.

In this previous study, it was demonstrated that L-cysteine can bind with Hg(II) ions and can also be modified on the surface of AuNPs. Therefore, the L-cysteine was used to modify on AuNPs surface for Hg(II) ions sensing in this study.

However, to improve the sensitivity of the method, the pre-concentration step can be useful. In many cases, the solid phase supports, such as resin [45], silica [46]

were used after surface modification with selective ligand for extraction of mercury from water samples. Examples are shown as follows.

Bagheri *et al.* [47] developed a method for determination of mercury(II) chloride ($HgCl_2$) and methyl-mercury ($MeHg^+$) in river water sample using on-line UV decomposition technique coupled with cold-vapor atomic fluorescence spectrometry (CV-AFS). All mercury species were pre-concentrated on silica gel modified with 2-mercaptobnzimidazol. To desorb mercury compounds, solutions of 0.05 M KCN and 2.0 M HCl was used to elute $HgCl_2$ and $MeHg^+$ species, respectively. Afterward, all mercury species were reduced with $SnCl_2$ solution and determined by CV-AFS technique. The detection limits of this method were 0.07 and 0.05 ng/L for mercury(II) chloride and methyl-mercury determination, respectively.

As shown above, silica was chosen as an efficient solid support as they has high specific surface area (700 -1,500 m^2/g) [48]. The silica surface could be modified with selective ligands for mercury extraction. In this study, we are interested in using silica modified with gold nanoparticles and L-cysteine for extraction and pre-concentration of Hg(II) ions in water samples.

CHAPTER III

EXPERIMENTAL

3.1 Apparatus

3.1.1 UV-Visible spectrophotometer (UV-Vis)

The localized surface plasmon resonance of gold nanoparticles solutions was observed by a UV-visible spectrophotometer (Hewlett-Packard, model 8453) using wavelengths ranging from 400 to 800 nm.

3.1.2 Cold-vapor atomic absorption spectrometer (CV-AAS)

The concentration of Hg(II) ions was measured by a cold-vapor atomic absorption spectrometer (Perkin Elmer, Analyst 100) coupled with a flow injection system (Perkin Elmer, FIAS 400) at the wavelength of 253.7 nm. The reduction of Hg(II) ions to Hg(0) vapor was achieved by using 1 % (w/v) $SnCl_2$ solution and 3 % (v/v) HCl solution.

3.1.3 Hot plate stirrer

Synthesis of gold nanoparticles solution was performed on a hot plate stirrer modelled IKA C-MAG HS 7.

3.1.4 Overhead shaker

Extraction of Hg(II) ions solution was carried out by shaking the mixture of solid phase and metal ions solution using an overhead shaker at 30 rpm.

3.2 Chemicals and reagents

All chemicals used in this research were analytical reagent grade and listed in Table 3.1.

Table 3.1 Chemicals list

Chemicals and reagents	Supplier
gold(III) chloride trihydrate (≥99.9%)	Sigma-Aldrich
Tri-sodium citrate dihydrate	Fisher Scientific
hexadecyltrimethylammonium bromide(≥96%)	Fluka
L-cysteine hydrochloride (≥98%)	Sigma-Aldrich
Mercury standard solution (1000 mg/L)	Fluka
Siver standard solution (1000 mg/L)	Merck
Asenic standard solution (1000 mg/L)	Merck
Cobalt standard solution (1000 mg/L)	Merck
Cadmium standard solution (1000 mg/L)	Merck
Cromium standard solution (1000 mg/L)	Merck
Copper standard solution (1000 mg/L)	Merck
Iron standard solution (1000 mg/L)	Merck
Manganese standard solution (1000 mg/L)	Merck
Nickel standard solution (1000 mg/L)	Merck
Lead standard solution (1000 mg/L)	Merck
Zinc standard solution (1000 mg/L)	Merck
Sodium chloride	Carlo Erba
Tin(II) chloride (98%)	Sigma-Aldrich
Hydrochloric acid (37%)	Merck

3.3 Preparation of chemicals and reagents solutions

All chemicals and reagents solutions were freshly prepared by using ultra-pure water (MilliQ).

3.3.1 Gold(III) ions solution

A 0.5 mM gold(III) ions solution was prepared by dissolving 19.7 mg of gold(III) chloride tri-hydrate in 100 mL of MilliQ water.

3.3.2 Citrate solution

A 0.5% (w/v) citrate solution was prepared by dissolving 0.5 g of tri-sodium citrate di-hydrate in 100 mL of MilliQ water. This solution was used to reduce gold(III) ions solution to gold nanoparticles.

3.3.3 Hexadecyl trimethyl ammonium bromide (CTAB) solution

A 0.2 M CTAB solution was prepared by dissolving 7.3 g of CTAB in 100 mL of MilliQ water. This solution was used to stabilize gold nanoparticles.

3.3.4 L-cysteine solution

A 25 mM L-cysteine solution was prepared by dissolving 0.4 g of L-cysteine hydrochloride in 100 mL of MilliQ water. This stock solution was diluted to desired concentrations using MilliQ water. These solutions were used to modify gold nanoparticles surface.

3.3.5 Mercury(II) standard solutions

Mercury standard solutions were prepared by diluting 1000 mg/L stock Hg(II) solution to desired concentrations using MilliQ water.

3.3.6 Sodium chloride solution

A 0.1 M sodium chloride solution was prepared by dissolving 5.8 g of sodium chloride in 100 mL of MilliQ water. This solution was used to the control ionic strength of the solution and produce anionic chloro complexes of Hg(II).

3.3.7 Tin(II) chloride solution

A Tin(II) chloride solution was prepared by dissolving 5 g of Tin(II) chloride in 400 mL of deionized water (DI water). Then, the solution was stirred about 30 minutes and mixed with 20 mL of conc. hydrochloric acid. Finally, the solution volume was adjusted to 500 mL using DI water. This solution was used as reducing agent for determination of Hg(II) ions by cold-vapor atomic absorption spectrometer (CV-AAS).

3.3.8 Hydrochloric acid

A 3% (v/v) hydrochloric acid solution was prepared by diluting 30 mL of hydrochloric acid in 1000 mL of DI water. This solution was used as carrier for determination of Hg(II) ions by cold-vapor atomic absorption spectrometer (CV-AAS).

3.4 Determination of mercury(II) ion by gold nanoparticles solution

3.4.1 Synthesis of gold nanoparticles solution

A gold nanoparticles solution (AuNPs) was prepared by reducing gold(III) chloride tri-hydrate ($HAuCl_4$) solution with tri-sodium citrate. A 20 mL of 0.5 mM $HAuCl_4$ solution was stirred and heated to a temperature between 85 and 90 $^\circ$C. Then, 2 mL of 0.5% (w/v) citrate solution was added into the $HAuCl_4$ solution and the mixture was kept at this temperature. The solution color changed from colorless to wine red within 15 minutes. The obtained AuNPs solution was stored in a glass bottle at 4°C for further use.

3.4.2 Optimization of determination of Hg(II) method

In this method, 1 mL of 0.15 mM AuNPs solution was mixed with 100 µL of 1.5 mM L-cysteine solution and 100 µL of NaCl solution of a specific concentration

for a specific modification time to produce cysteine modified AuNPs (cys-AuNPs). Then, Hg(II) solution (5 or 10 μg/L) of a specific volume was added into the cys-AuNPs solution and mixed for a certain time (detection time) before detection by UV-Visible spectrophotometer. Under a optimized condition, all process were performed again to investigate the effect of other ions by using a binary mixture of another ion and Hg(II) ion and compared with a single solution of Hg(II). Afterward, the accuracy and detection limit of the method was evaluated by comparing with those of cold-vapor atomic absorption spectrophotometer (CV-AAS). Finally, the method was applied to determine Hg(II) ions in real water samples (drinking and tap water). The concept of the method was illustrated in Figure 3.1.
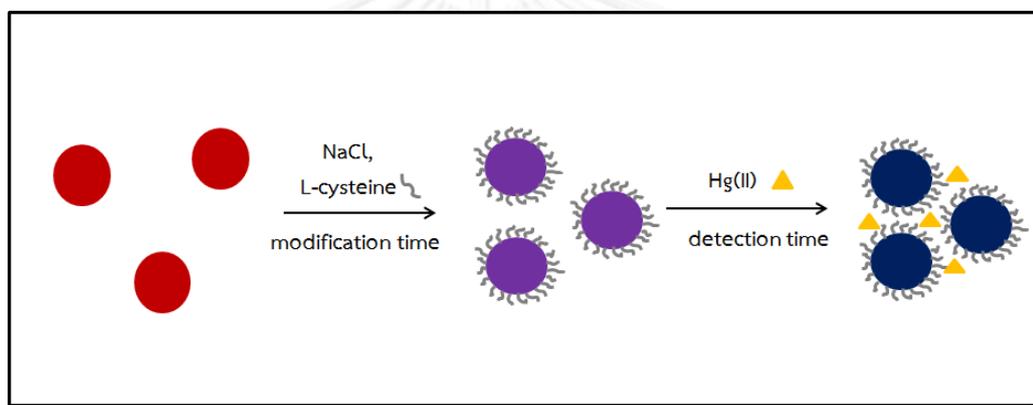
Figure 3.1 Scheme of the purposed method of Hg(II) ion determination by gold nanoparticles solution.

3.4.2.1 Effect of modification time

Gold nanoparticles were modified with L-cysteine (cys) by adding 100 μL of 1.5 mM L-cysteine and 100 μL of 0.05 M NaCl into 1.00 mL of 0.15 mM AuNPs solution. The spectra of cys-AuNPs solution were observed after 1 to 20 minutes using UV-Visible spectrophotometer (UV-Vis).

3.4.2.2 Effect of sodium chloride

All water samples normally contain many ions from various salts. These ions may interfere the determination of Hg(II) ions, in particular cations could also induce the aggregation of citrate capped AuNPs. Sodium and chloride ions are the two of major ions found in water. Therefore, to control the ionic strength of the solution so

that salt from sample would not significantly affect the aggregation, NaCl chosen as representative of salts was added to the solution. 100 µL of NaCl of various concentration ranging from 0.01 to 0.1 M were added into the mixture of 0.15 mM AuNPs and 1.5 mM L-cysteine during the surface modification step (10 minutes of modification time).

3.4.2.3 Effect of detection time

To find a suitable time for detection of Hg(II) ions, the time for cys-AuNPs to aggregate with Hg(II) ions was monitored at 1 to 20 minutes by UV-Visible spectrophotometer. Its absorbance signal was investigated against MilliQ water which was the reagent blank. Two concentrations of Hg(II) ions solution (5 and 10 µg/L) were applied. The concentration of AuNPs and L-cysteine solution were maintained at 0.15 and 1.5 mM, respectively. The modification time between AuNPs and L-cysteine solution was 10 minutes.

3.4.2.4 Effect of sample volume

In order to obtain a suitable sample volume for the determination of Hg(II) ions, sample volume in a range of 50 to 200 µL was used. The Hg(II) solutions of 5 and 10 µg/L were prepared and used as sample solutions. The aggregation of cys-AuNPs induced by Hg(II) ions was monitored by UV-Visible spectrophotometer. Its absorbance signal was read against that of the reagent blank, MilliQ water. The concentration of AuNPs and L-cysteine solution were fixed at 0.15 and 1.5 mM, respectively. The modification and detection time of 10 and 20 minutes, respectively were adopted.

3.4.2.5 Effect of co-existing ions

The effect of co-existing ions was observed by analyzing a binary mixture solution of Hg(II) and another metal ion (Ag(I), As(III), Co(II), Cd(II), Cr(III), Cu(II), Fe(III), Mn(II), Pb(II) or Zn(II)) at a Hg(II) ion : metal ion mole ratio of 1:100 by cys-AuNPs solution. The absorbance of the solution was measured by UV-Visible spectrophotometer at 520 and 670 nm. Its absorbance signal was compared to that of a single Hg(II) solution. The concentrations of AuNPs and L-cysteine solution were

kept at 0.15 and 1.5 mM, respectively. The modification and detection time of 10 and 20 minutes were used, respectively

3.4.3 Evaluation of method performance

To evaluate method performance, Hg(II) standard solutions at concentrations in the range of 5 to 40 µg/L were analyzed. The analysis was repeated at least 3 times. A calibration curve was constructed by plotting the value of absorbance ratio at 670 and 520 nm against Hg(II) concentration levels. The limit of detection was obtained by comparing the signal calculated by following eq. 3.1 to the calibration curve. S.D. was the standard deviation of blank signals.

LOD = signal of reagent blank + 3(S.D.) (3.1)

To evaluate the accuracy of method, a standard solution of 10 µg/L Hg(II) ions was spiked into the drinking and tap water. The absorbance ratio was calculated and the concentration obtained was compared with the value observed by CV-AAS. The accuracy of method was monitored as percentage of recovery that could be calculated from the following equation 3.2,

$$\% \text{ recovery} = \frac{(Xs - Xb)}{S} \times 100 \qquad (3.2)$$

Where Xs = the mass of Hg(II) ions found in spiked sample

Xb = the mass of Hg(II) ions found in non-spiked sample

S   = the mass of Hg(II) ions spiked in the sample

3.5 Determination of mercury(II) ion by gold nanoparticles on silica

3.5.1 Synthesis of gold nanoparticles

A gold nanoparticles solution was prepared as described in detail in section 3.4.1. The 10 ml of 0.2 M hexadecyl trimethyl ammonium bromide solution (CTAB) was added to the obtained AuNPs solution in order to stabilize AuNPs with CTAB. The mixture solution was stirred about 1 hour before keeping for further use.

3.5.2 Optimization of Hg(II) determination method

The method for Hg(II) detection is illustrated in Figure 3.2. To prepare solid phase for Hg(II) detection (AuNPs-Si), 1 mL AuNPs of a specific concentration was added into 0.1 g silica, mixed for a specific coating time and washed with MilliQ water to remove unattached and loosely attached AuNPs. Then, 1 mL L-cysteine solution of a specific concentration was added into AuNPs-Si phase and mixed for 10 minutes before washing with MilliQ water to remove unmodified L-cysteine. On the other hand, 1 mL of 0.1 M NaCl solution was added into standard or sample solution to form chloro complexes with Hg(II) ions and the 10 mL of standard or sample solution were extracted during a specific extraction time by cys-AuNPs-Si and washed with millQ water. Finally, the Hg(II) ion adsorbed on cys-AuNPs-Si was reduced with 1 mL of $SnCl_2$ of specific concentration for 30 minutes. The color of the solid was observed by naked eyes compared to a solid blank. The concentration of Hg(II) in a range of 2 -100 µg/L was studied. Under a suitable condition, all processes were done again to investigate the effect of other metal ions by using a binary mixture solution of another ion and Hg(II) ion (the mole ratio of Hg(II) : another ion at 1 : 100) and compared to single Hg(II) ions solution. Finally, the method was applied to detect Hg(II) ions in real water samples (drinking and tap water).
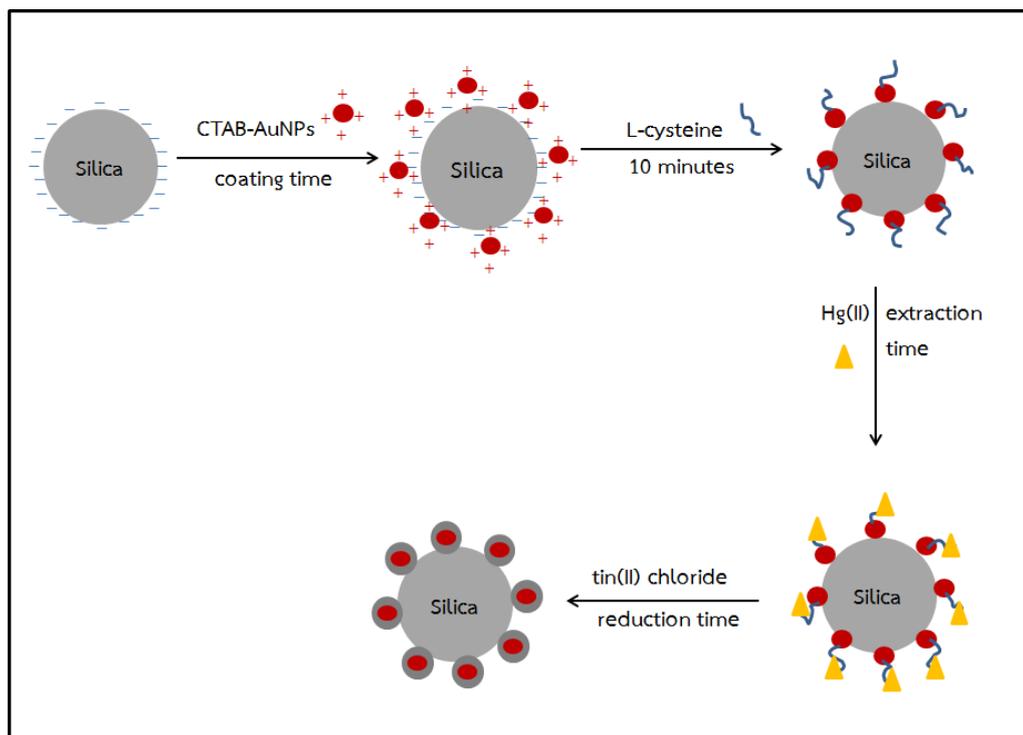
Figure 3.2 Scheme of the purposed method of Hg(II) ion determination by cysteine modified AuNPs supported silica.

3.5.2.1 Effect of gold nanoparticles concentration and coating time

To prepare AuNPs supported silica (AuNPs-Si) for Hg(II) extraction and determination, silica gel was coated with gold nanoparticle solution. Different concentrations of the AuNPs solution ranging from 0.1 to 0.5 M were prepared. The 1 mL of AuNPs solution of various solution was mixed with 0.1 g of silica for different contact times (5-30 minutes). Then, the AuNPs-Si phases were washed three times with milliQ water to remove loosely attached AuNPs. Afterward, the color of all AuNPs-Si phases prepared with different AuNPs concentrations and different contact times was observed by necked eyes. Its color was monitored before and after the phase washing with MilliQ water. A suitable AuNPs concentration and contact time should yield phase that has a stable and distinct color after washing with MilliQ water for an ease in color observation during Hg(II) ion extraction and reduction.

3.5.2.2 Effect of L-cysteine concentration

In order to obtain a suitable L-cysteine concentration for modifying AuNPs supported silica, various concentrations of L-cysteine solution ranging from 5 to 25 mM were used. The 1 mL of L-cysteine solution was added into 0.1 g of AuNPs-Si and stirred for 10 minutes. Then, the AuNPs-Si modified with L-cysteine (cys-AuNPs-Si) was washed three times with milliQ water to remove unattached L-cysteine. Afterward, the cys-AuNPs-Si phases were used in the extraction of 10 mL of solution containing 2 to 100 µg/L Hg(II). Then, the obtained phases were washed three times with milliQ water. Furthermore, the extracted Hg(II) ions on the solid phase were reduced with 1.0 mL of 0.01 M $SnCl_2$. Its color was monitored by necked eyes at 30 minutes of the reducing time. In this experiment, the time in silica gel coating with AuNPs and Hg(II) ions extraction were fixed at 30 minutes. The AuNPs and L-cysteine concentrations were 0.5 and 10 mM, respectively.

3.5.2.3 Effect of extraction time

The time for Hg(II) extraction by cys-AuNPs-Si phase was varied in the range of 5 to 30 minutes and Hg(II) solutions (10.00 mL) with concentration ranging from 2 to 100 µg/l were applied. After extraction, the solid phases were washed three times. The solid phase color was monitored by necked eyes when the extracted Hg(II) on the solid phase were reduced with 0.01 M $SnCl_2$ for 30minutes. Meanwhile, the coating time was maintained at 30 minutes. The solution of AuNPs and L-cysteine with concentration of 0.5 and 5 mM were used, respectively.

3.5.2.4 Effect of tin(II) chloride concentration

In order to find a suitable tin(II) chloride concentration for Hg(II) ions reduction, $SnCl_2$ solution of various concentration ranging from 0.001 to 0.1 M were prepared and applied to reduce Hg(II) extracted from solutions of different concentration (2 - 100 µg/L). Its color was monitored by necked eyes at 30 minutes of reducing time. Meanwhile, the coating and extraction time were maintained at 30 minutes. The solution of AuNPs and L-cysteine with concentration of 0.5 and 5 mM, respectively were used.

3.5.2.5 Effect of co-existing ions

The effect of co-existing ions was investigated by adding a solution of single metal ions (Ag(I), As(III), Co(II), Cd(II), Cr(III), Cu(II), Fe(III), Mn(II), Pb(II) or Zn(II)) to the cys-AuNPs-Si phase. The color of solid phase was observed before and after reduction with 0.01 M $SnCl_2$ by necked eyes and compared against Hg extracted solid phase. Meanwhile, the coating, extraction and reduction time were maintained at 30 minutes. The solution of AuNPs and L-cysteine with concentration of 0.5 and 5 mM, respectively were used.

3.5.3 The method performance

To evaluate the method performance, the solid phase was used to detect Hg(II) ions in a spiked sample under the suitable experimental condition. The 10 μg/L of Hg(II) were spiked into the drinking and tap water samples. Their colors were observed and compared to 10 μg/L of Hg(II) standard solution and non-spiked samples.

CHAPTER IV

RESULTS AND DISCUSSION

In this chapter, methods for determination of Hg(II) ion by gold nanoparticles are proposed. The first method follows the aggregation of L-cysteine modified-gold nanoparticles (cys-AuNPs) in solution induced by Hg(II) ions and determination by UV-Vis spectrophotometry. The second method focuses on the use of L-cysteine modified gold nanoparticles coated silica gel as solid phase for extraction and determination of mercury by naked eyes after reducing the attached Hg(II) ions to elemental mercury that would form amalgam with AuNPs on silica phase.

4.1 Determination of mercury(II) ion by gold nanoparticles solution

4.1.1. Reaction between modified AuNPs and Hg(II) ions in solution

A gold nanoparticle (AuNPs) solution was prepared by reducing Au(III) ions with citrate. The coverage of citrate anions on the AuNPs surface could stabilize the colloidal AuNPs for about 7 days. The color of the AuNPs solution was wine-red and the characteristic surface plasmon resonance (SPR) band of this solution was observed by UV-Visible spectrophotometer. An SPR band with λ_{max} at 520 nm was observed corresponding to the SPR band of AuNPs of 13 nm in diameter. After the addition of L-cysteine into the AuNPs solution, the solution color was changed from wine-red to dark purple, resulting in the red shift of λ_{max} due to the adsorption of L-cysteine on AuNPs surface, resulting in less stable AuNPs that eventually aggregated together. In the presence of Hg(II) ions that could form complexes with L-cysteine, the aggregation of cys-AuNPs occurred and the red shift of λ_{max} was observed (Figure 4.1). The SPR band with λ_{520} was related to the signal of small particles, whereas the band at 670 nm corresponded to the signal of AuNPs aggregates. The change of AuNPs inter-particle distance induced by the presence of Hg(II) ions was monitored by using the absorbance ratio at 670 nm to 520 nm ($A_{670/520}$).
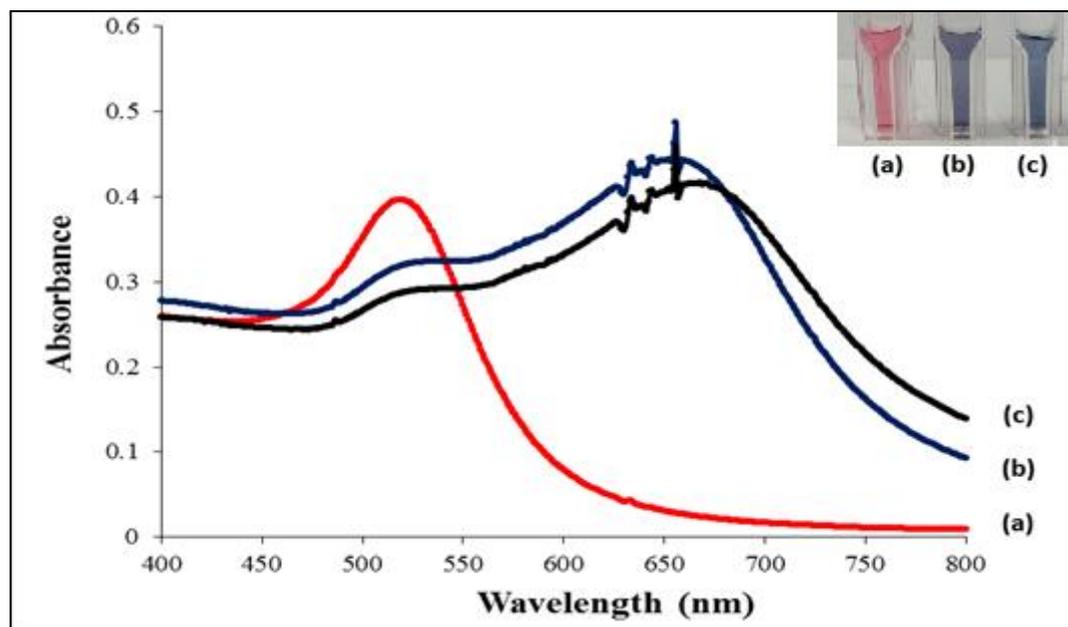
Figure 4.1 UV-Visible spectra and solution of (a) AuNPs, (b) cys-AuNPs and (c) cys-AuNPs + Hg(II) (40µg/L); detection time = 20 min, C_{NaCl} = 0.05M.

4.1.2 Determination of Hg(II) by cys-AuNPs solution

The steps in the determination of Hg(II) by AuNPs and UV-Vis spectrophotometer was illustrated in Figure 4.2. L-cysteine was added into the AuNPs solution to modify the AuNPs surface (cys-AuNPs) for a specific period of time (modification time). Afterward, the cys-AuNPs solution was mixed with an Hg(II) standard solution or sample for a certain period of time (detection time) prior to the analysis by UV-Visible spectrophotometer. The effects of modification time, sodium chloride, detection time, sample volume and co-existing ions were investigated. Based on the change of AuNPs inter-particle distance induced by Hg(II) ions, the particle aggregation was monitored using the absorbance ratio at 670 nm to 520 nm ($A_{670/520}$).
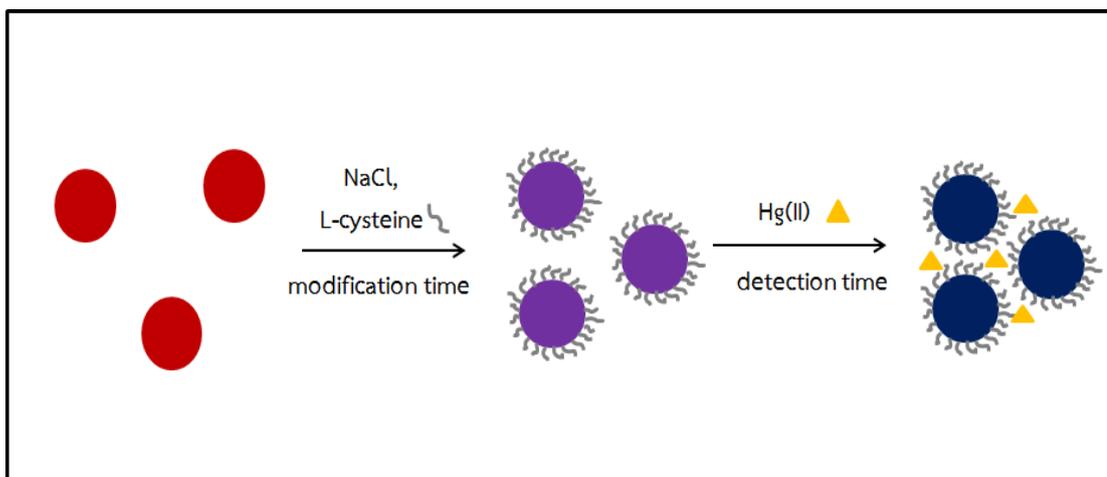
Figure 4.2 **The steps of Hg(II) detection by AuNPs solution**

In the preliminary study, it was found that the concentrations of AuNPs and L-cysteine of higher than 0.15 and 1.5 mM, respectively, did not lead to a significant change of the absorbance ratio at 670 nm to 520 nm ($A_{670/520}$) in the presence of Hg(II) ions. It is likely that under the condition of high AuNPs and L-cysteine concentrations, large cys-AuNPs aggregate was obtained prior to the addition of Hg(II) ions and, hence the presence of Hg(II) ions at low concentration could not induce the formation of larger cys-AuNPs aggregates. Therefore, the concentrations of AuNPs and L-cysteine of 0.15 and 1.5 mM, respectively were chosen in this method.

4.1.2.1 Effect of modification time

In the preliminary study, it was found that degree of the aggregation of AuNPs with L-cysteine depended on the contact time between AuNPs and L-cysteine (modification time). Therefore, in order to obtain a suitable modification time, the aggregation of AuNPs with L-cysteine was observed at a modification time varied from 1 to 20 minutes. Based on the results shown in Figure 4.3, the value of $A_{670/520}$ was low at the starting time and then, rapidly increased and reached a relatively constant value within 10 minutes. It could be explained that the aggregation of cys-AuNPs occurred continuously resulting in an increase in absorbance at 670 nm and a decrease in absorbance at 520 nm. The process reached equilibrium within 10 minutes as no significant change in $A_{670/520}$ values was observed. Therefore, the chosen modification time for next experiments was 10 minutes.
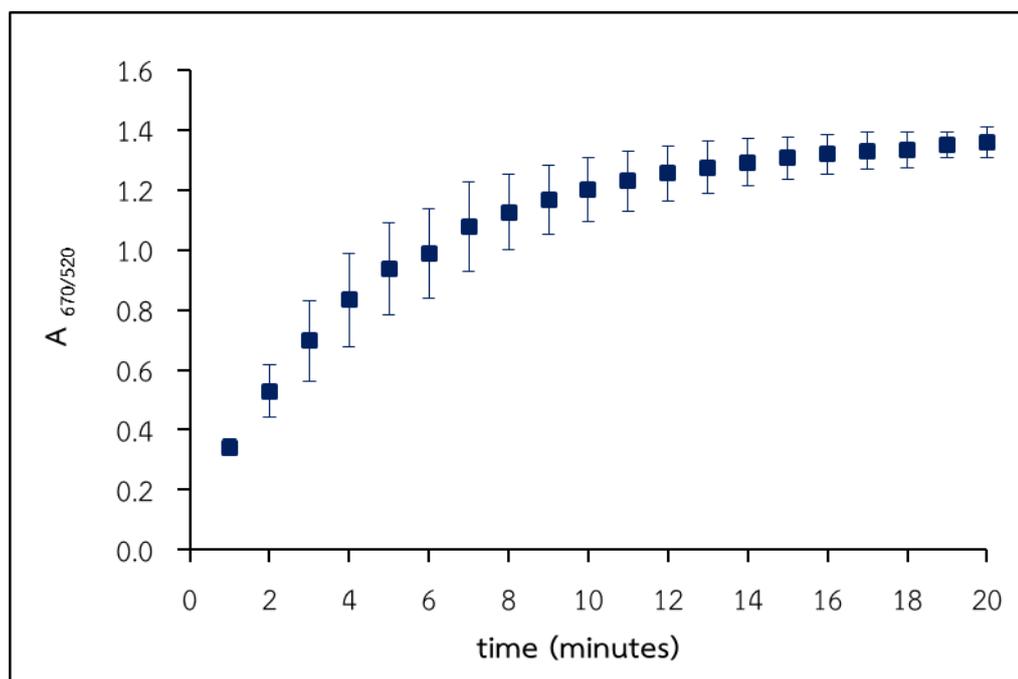
Figure 4.3 The absorbance ratio 670/520 nm of cys-AuNPs solution ($A_{670/520}$) under different modification times; C_{NaCl} = 0.05 M.

4.1.2.2 Effect of sodium chloride

In water samples, the presence of other ions, in particular cations may interfere the aggregation of cys-AuNPs due to the balance of negative charges of citrate capped AuNPs. As consequence, the aggregation of cys-AuNPs would not only be induced by Hg(II) ions, but also by other cations. Therefore, it is necessary to control ionic strength of the system so that the effect of additional ions from sample would be negligible. To simulate the condition in water samples, NaCl was chosen for this purpose. According to Ministry of public health (Thailand), the chloride level in drinking water should not exceed 250-600 mg/L (~0.007-0.017 M). Meanwhile, the chloride concentration in tap water should not be also higher than 250-600 mg/L (~0.007-0.017 M). In this study, the concentration of NaCl was varied in the range of 0.01 to 0.5 M and added into the solution mixture of 0.15 mM AuNPs and 1.5 mM L-cysteine during the AuNPs modification step. In Figure 4.4, it shows that the low value of $A_{670/520}$ was observed in the presence of NaCl at low concentrations at the beginning, indicating a low degree of cys-AuNPs aggregation. The $A_{670/520}$ value increased when the concentration of NaCl was increased because of higher degree of aggregation. The equilibrium of aggregation process was achieved when 0.05 M of

NaCl or higher concentrations was used. Therefore, 0.05 M NaCl solution was chosen to control the ionic strength of solution.
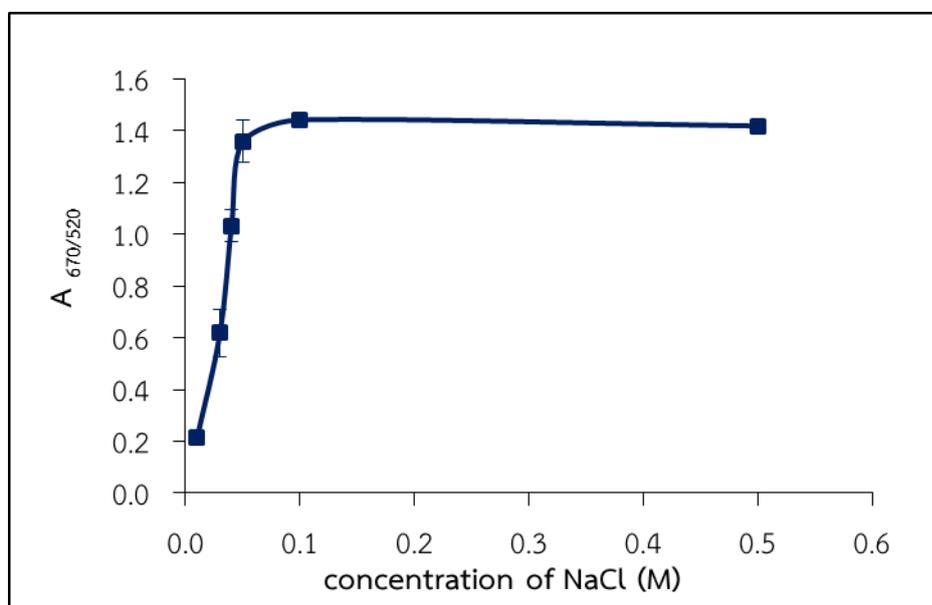
Figure 4.4 **The absorbance ratio 670/520 nm of cys-AuNPs solution ($A_{670/520}$) in the presence of different NaCl concentrations; modification time = 10 min.**

4.1.2.3 Effect of detection time

To investigate the effect of detection time, the aggregation of the cys-AuNPs solutions induced by Hg(II) ions was followed using detection time in the range of 1 to 20 minutes. From Figure 4.5, the values of $A_{670/520}$ of two concentration of Hg(II) ions (5 and 10 µg/L) were compared to those of the reagent blank. The longer the detection time, the higher value of $A_{670/520}$ was obtained. A significant difference in $A_{670/520}$ values of various Hg(II) standard solutions was observed at the detection time of 18 minutes and the largest difference in their $A_{670/520}$ values was achieved at the detection time of 20 minutes. It could be explained that Hg(II) ions of both concentrations aggregated quickly with cys-AuNPs in the earliest stage. Afterward, the aggregation slowed down and reached its highest degree of aggregation which were different due to different amount of Hg(II) ions. Therefore, the time for Hg(II) detection of 20 minutes was chosen.
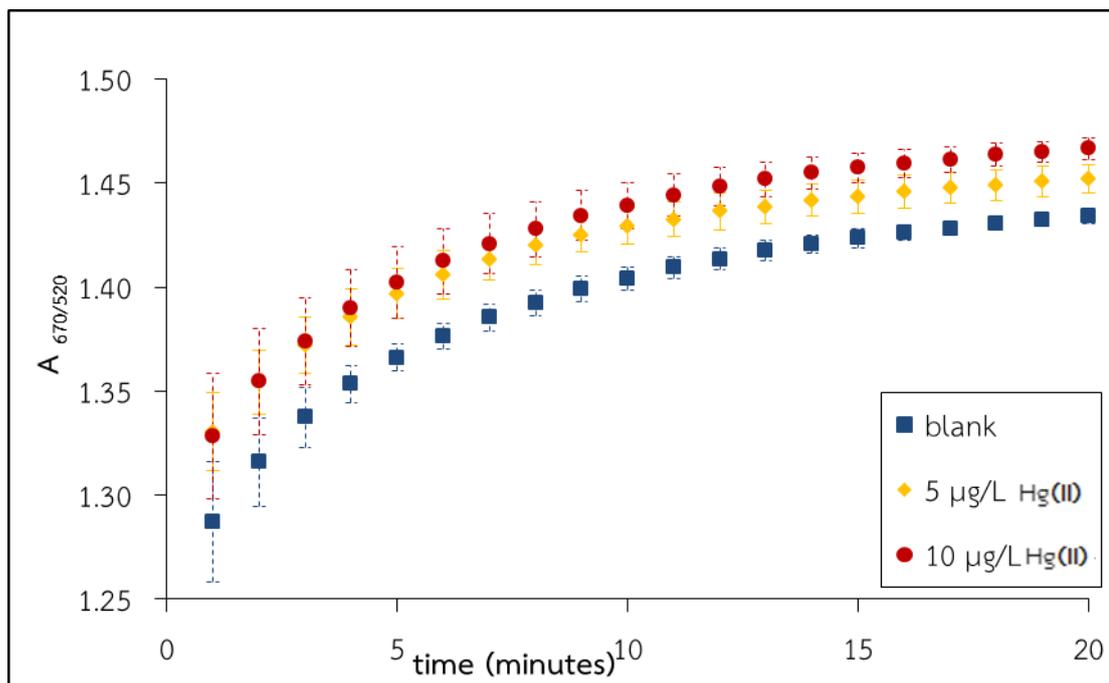
Figure 4.5 **The absorbance ratio 670/520 nm of cys-AuNPs solution ($A_{670/520}$) in the presence and absence of Hg(II) ions under different detection times; modification time = 10 min, C_{NaCl} = 0.05M.**

4.1.2.4 Effect of sample volume

In water samples, the co-existing ions or substances may interfere the determination of Hg(II) by cys-AuNPs. Sample volume could be reduced in order to reduce the matrix interference effect; however, a good sensitivity in the determination should be maintained. In this section, the sample volume of 50, 100 and 200 µL were chosen for the experiments. As shown in Figure 4.6, in a 50 µL sample system, the higher the concentration of Hg(II), the higher $A_{670/520}$ values were observed. On the other hand, the $A_{670/520}$ values in the 100 µL and 200 µL sample systems did not show a reasonable trend with respect to Hg(II) concentration. It was probably due to a large and excess amount of Hg(II) ions in samples, compared to cys-AuNPs in the solution and therefore, there was no difference in the degree of aggregation in the presence of Hg(II) of different concentrations. Thus, a suitable sample volume for Hg(II) detection was 50 µL.
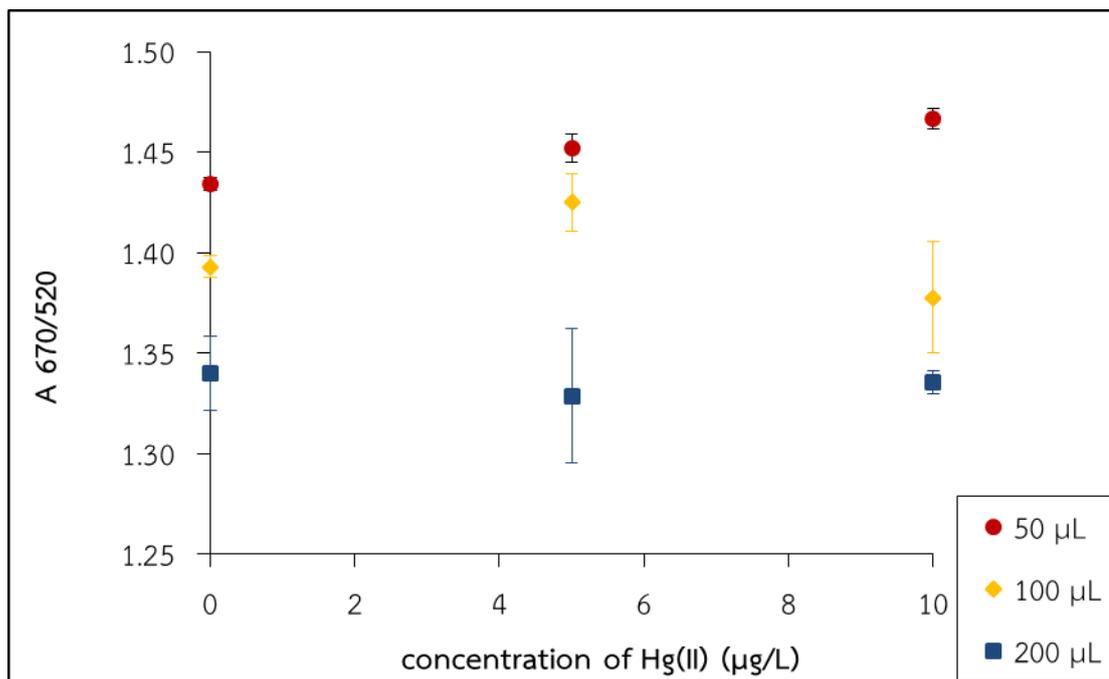
Figure 4.6 The absorbance ratio 670/520 nm of cys-AuNPs solution ($A_{670/520}$) under different Hg(II) solution volumes; detection time = 20 min, C_{NaCl} = 0.05M.

4.1.2.5 Effect of other heavy metal ions

To investigate the effect of potential interfering metal ions, the absorbance signal of binary mixture solutions between Hg(II) and other metal ions (Ag(I), As(III), Co(II), Cd(II), Cr(III), Cu(II), Fe(III), Mn(II), Ni(II), Pb(II) or Zn(II)) at a mole ratio of 1:100 was observed at 520 and 670 nm. Its absorbance signal was read and compared to that observed from a single Hg(II) solution. From Figure 4.7, it can be seen that all metal ions did not affect the Hg(II) detection because $A_{670/520}$ values of all binary mixtures and single Hg(II) solution were no significantly different. Hence, the method had a high selectivity in Hg(II) detection.
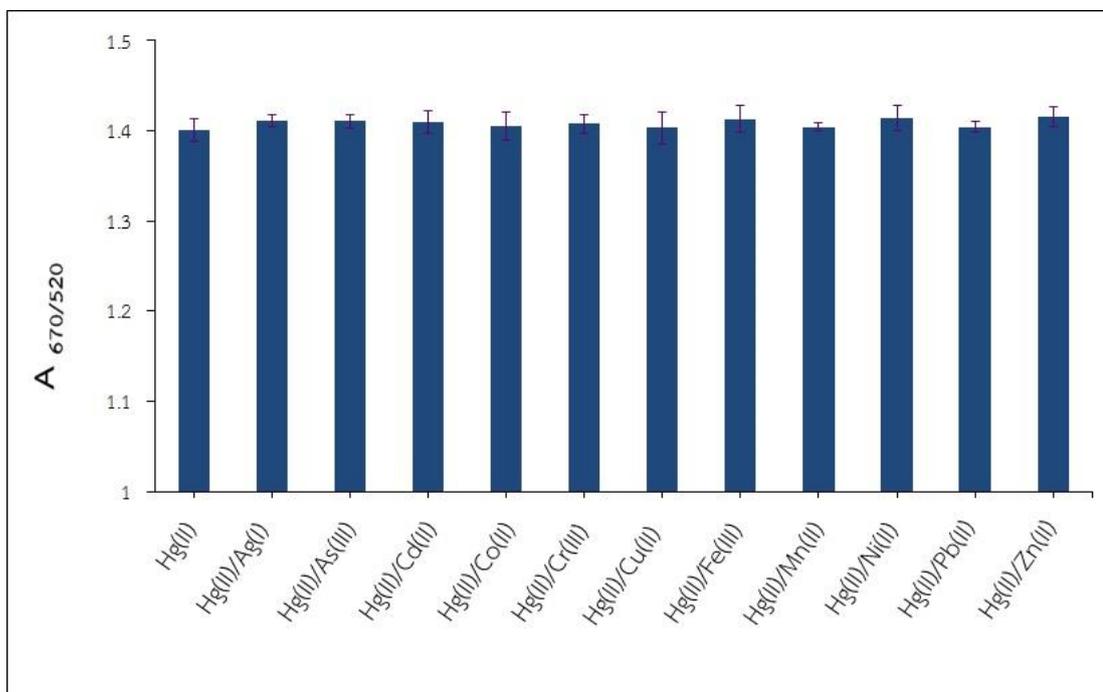
Figure 4.7 **The absorbance ratio 670/520 nm (A$_{670/520}$) of single Hg(II) solution and binary mixture solution of Hg(II) (0.025μM) and various metal ions (2.5 μM).**

4.1.3 Method performance

Under the suitable condition, a calibration curve between the values of A$_{670/520}$ and Hg(II) concentration was built using Hg(II) ion solution with concentrations ranging from 5 to 40 μg/L. Based on results in Figure 4.8, a linear relationship was obtained (R^2 = 0.9894). The limit of Hg(II) ion detection using spectrophotometry was 4.5 μg/L.
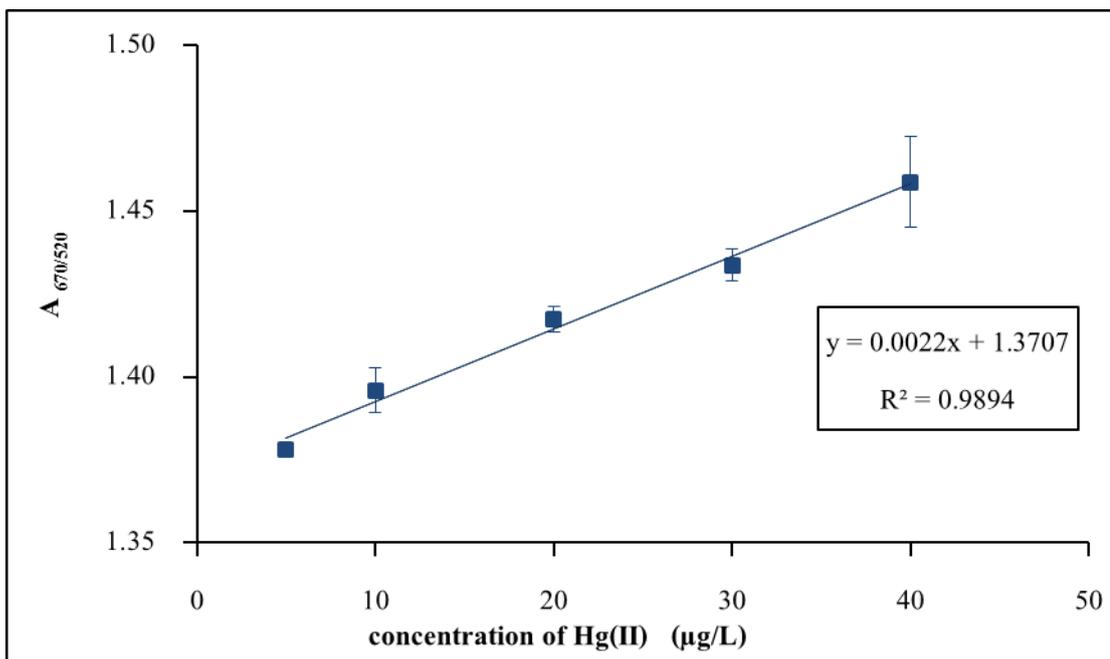
Figure 4.8 The standard curve for Hg(II) determination.

The accuracy of this method was appraised by determining the samples (drinking water, tap water) spiked with 10 µg/L Hg(II) standard solution (Table 4.1). The percentage of recovery was calculated by comparing with non-spiked samples. Results from drinking water analysis obtained from the AuNPs method (11.17 µg/L, 111.7%) were close to those observed by a cold vapor-atomic absorption spectrometer (CV-AAS) (11.66 µg/L), revealing that the method has acceptable accuracy. However, in tap water analysis by the AuNPs method, the large $A_{670/520}$ value of the non-spiked sample was observed possibly due to matrix interfering effect, while the amount of Hg(II) in the same sample was non-detectable by CV-AAS. These results indicate that the proposed AuNPs method still needs more investigation to overcome the matrix effect.

Table 4.1 Determination of Hg(II) in water sample (n=3)

Type of water	Hg(II) ions (µg/L) (added)	Hg(II) ions (µg/L) (found)	
		AuNPs method	Standard method (CV-AAS)
Drinking water	0	ND	ND
	10	11.17± 0.10	11.66 ± 0.02
Tap water	0	40.45 ± 0.30	ND
	10	51.15 ± 0.85	11.92 ± 0.04

4.2 Determination of Hg(II) by L-cysteine modified AuNPs supported silica

In this section, a gold nanoparticl solution was prepared by reducing Au(III) ions with citrate. Then, the AuNPs solution was stabilized by CTAB for covering AuNPs surface with CTAB cations. The colloidal AuNPs particles were taken to coat on silica phase, which could have negative charge on the surface due to the dissociation of silanol groups, to produce AuNPs supported silica (AuNPs-Si). Next, the solid phase was washed to remove unattached and loosely attached AuNPs particles. Afterward, the AuNPs-Si phase was modified with L-cysteine via electrostatic interaction between the cations of CTAB on AuNPs surface and the anions of carboxylic group in L-cysteine. Then, Hg(II) ions in standard solutions or samples were extracted by cys-AuNPs-Si phase and finally, the Hg(II) ions adsorbed on the solid phase was reduced to Hg(0) by $SnCl_2$ and formed amalgam with AuNPs under suitable condition. The change of phase color was observed by necked eyes. The process was shown in Figure 4.9.
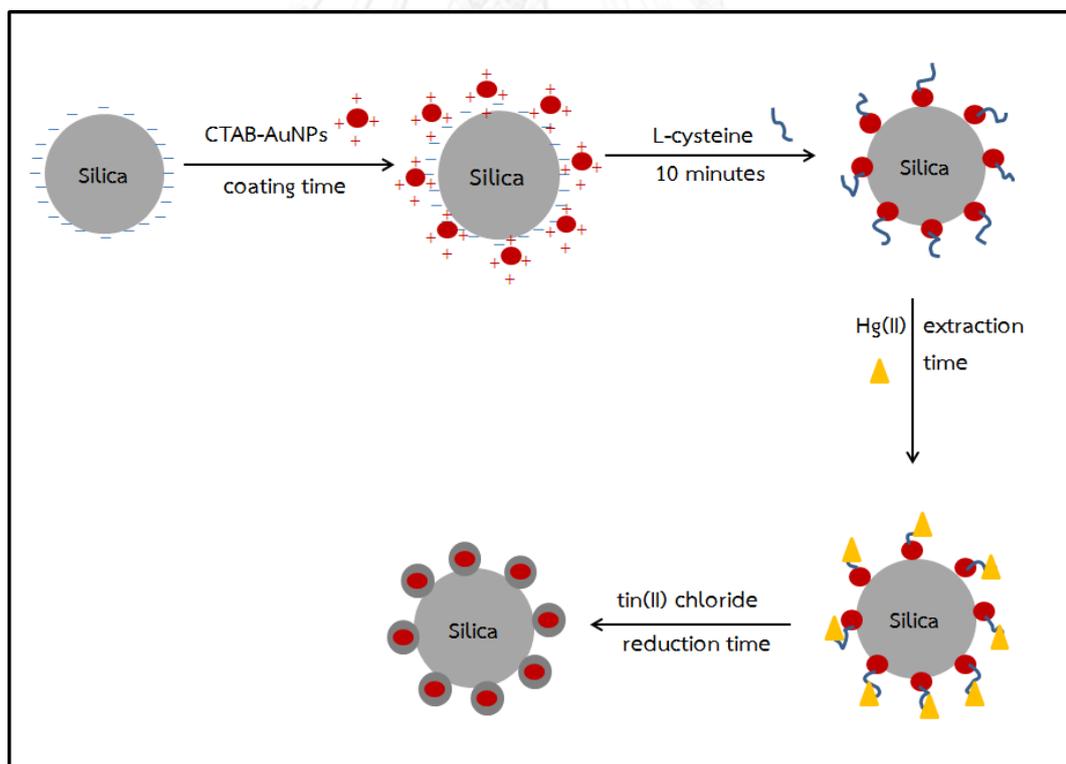
Figure 4.9 Scheme of the purposed method of Hg(II) ion determination by L-cysteine modified AuNPs supported silica.

4.2.1 Effect of gold nanoparticles concentration and coating time

To investigate the effect of gold nanoparticles concentration and coating time, different concentrations of AuNPs in range of 0.1 to 0.5 mM were used to coat a silica phase under various coating times in the range of 5 to 30 minutes. As shown with Figure 4.10, the color of solid phase changed from white color of silica to light pink and darker pink when increasing the concentration of AuNPs and the solid phase had a distinct color at 0.5 M AuNPs. Furthermore, the higher AuNPs content on the silica phase, the larger number of sites for L-cysteine modification and Hg(II) extraction were obtained. Thus, the AuNPs concentration of 0.5 M was chosen for further experiment because the color change could be observed easily.

On the other hand, the coating time also affected the coating of AuNPs onto silica phase as observed in Figure 4.10. Using the same concentration of AuNPs, the color of solid phase was more intense with longer coating time. Nevertheless, AuNPs could be detached from silica surface during washing process when the solid phase was prepared with contact time in a range of 5 to 25 minutes, revealing that the adsorption of AuNPs onto silica did not reach its equilibrium. Therefore, the suitable coating time was 30 minutes.
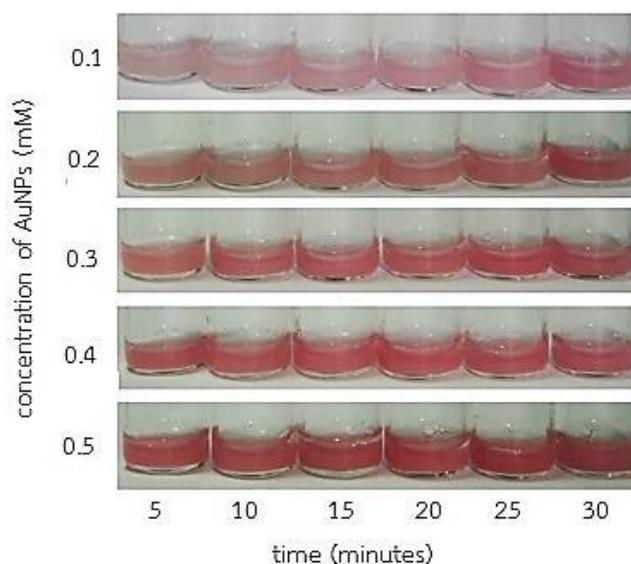
Figure 4.10 **The solid phase color after adding 0.1 to 0.5 mM AuNPs observed at different coating times.**

4.2.2Effect of L-cysteine concentration

In order to find a suitable L-cysteine concentration for AuNPs-Si modification, solutions containing Hg(II) in the range of 2 to 100 µg/L were used in the experiments and the color of cys-AuNPs-Si phase prepared with different L-cysteine concentration was observed after Hg(II) extraction and reduction. From Figure 4.11, using cys-AgNPs-Si phase prepared with 5 mM of L-cysteine, the color of the solid phase did not noticeably change when the concentration of Hg(II) increased it might be due to an insufficient amount of L-cysteine on cys-AgNPs-Si phase for Hg(II) extraction. On the other hand, the phase prepared with 10 mM of L-cysteine showed the color change from pink to blue when the concentration of Hg(II) increased. In the higher L-cysteine concentration system, the color of all solid phase was not different in increasing Hg(II) concentration Thus, the suitable concentration of L-cysteine for AuNPs-Si modification for Hg(II) detection was 10 mM.
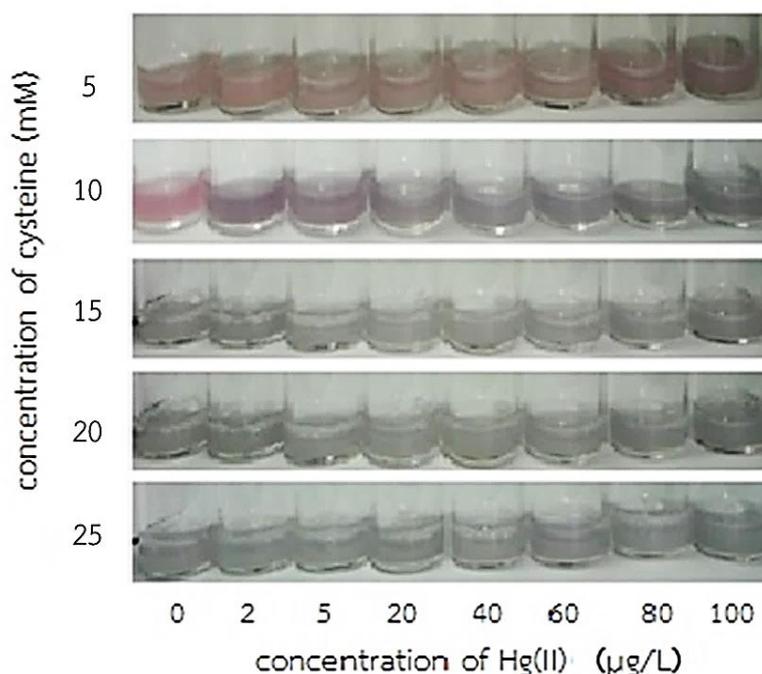
Figure 4.11 The color of solid phase prepared by using 5 to 25 mM L-cysteine after extraction of Hg(II) (2-100 µg/L) and reduction with 0.01 M SnCl$_2$ under the coating time : 30 minutes; extraction time : 30 minutes; reduction time: 30 minutes.

4.2.3 Effect of extraction time

To investigate the effect of extraction time, solutions containing Hg(II) in the range of 2 to 100 µg/L were used in the experiments and the color of cys-AuNPs-Si phase was observed after Hg(II) extraction with different extraction time and. Based on results in Figure 4.12, the color of solid phase after Hg(II) extraction was different from the one served as blank (which was in contact with only milliQ water) for all extraction times. After reducing Hg(II) on solid phase with 0.01 M SnCl$_2$, the difference in solid phase colors used to extract various concentrations of Hg(II) was clearly observed when longer contact time was applied. It was because higher amount of Hg(II) could be extracted. Therefore, the extraction time of 30 minutes was chosen for Hg(II) detection.
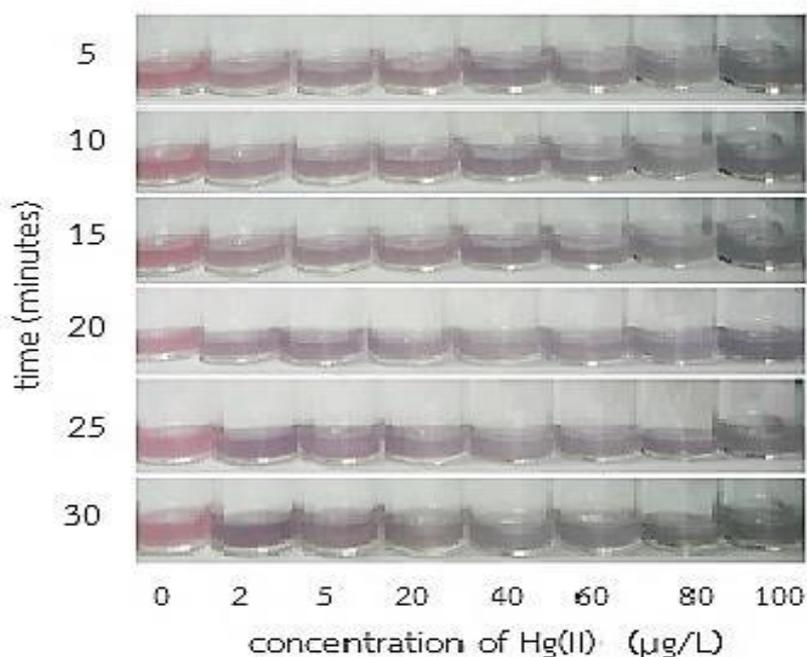
Figure 4.12 **The solid phase color after extraction of Hg(II) (2-100 µg/L) and reduction with 0.01 M SnCl$_2$ under different extraction time (5-30 minutes); coating time : 30 minutes; reduction time : 30 minutes.**

4.2.4 Effect of tin(II) chloride concentration

To investigate the effect of tin(II) chloride concentration, different $SnCl_2$ concentration in the range of 0.001 to 0.1 M were used to reduce the Hg(II) ions extracted from standard solutions (2-100 µg/L) by the solid phase. As shown in Figure 4.13, the solid phase after Hg(II) reduction had distinct color when the concentration of $SnCl_2$ increased from 0.001 to 0.01 M. However, the solid phase color in the presence of Hg(II) was colorless when reduced them with $SnCl_2$ >0.01 M.
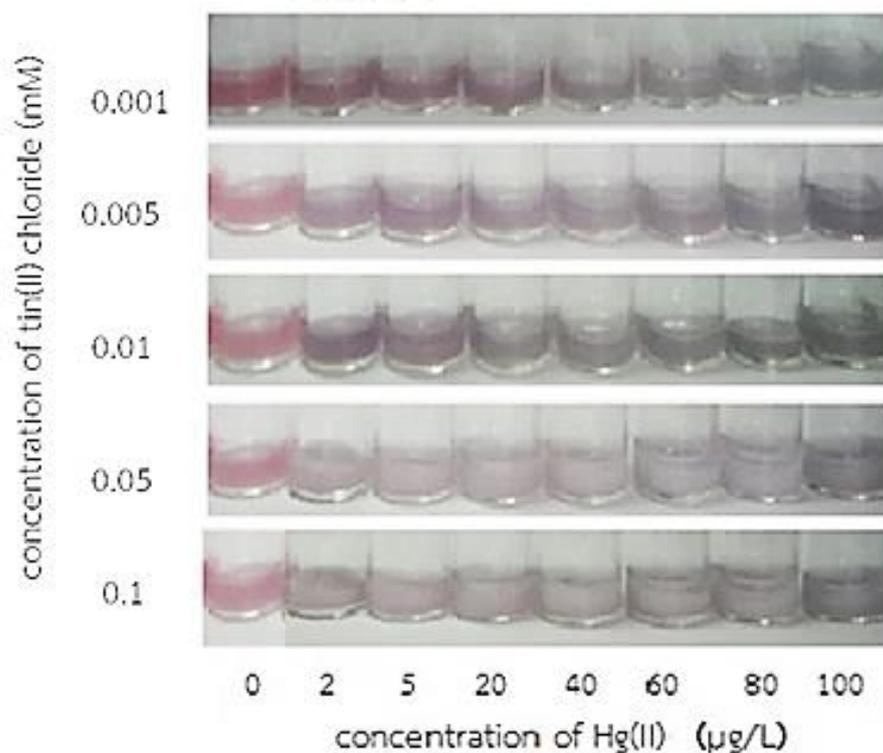
Figure 4.13 **The solid phase color after extraction of Hg(II) (2-100 µg/L) and reduction with SnCl$_2$ of different concentration; extraction time : 30 minutes, coating time : 30 minutes, reduction time : 30 minutes.**

4.2.5 Effect of other heavy metal ions

The effect of co-existing ions was studied by observing the color of cys-AgNPs-Si phase after extraction and reduction of other metal ions (Ag(I), As(III), Co(II), Cd(II), Cr(III), Cu(II), Fe(III), Mn(II), Ni(II), Pb(II) or Zn(II)) and comparing to Hg(II) ions system. The concentration of the other metal ions was 100 times higher than that of Hg(II) ions. The results in Figure 4.14 show that all other metal ions did not give

positive response and hence would not interfere Hg(II) detection. These results indicate that the proposed method has a high selectivity in Hg(II) detection.

AuNPs-Si Ag(I) As(III) Co(II) Cd(II) Cr(III) Cu(II) Fe(III) Hg(II) Mn(II) Ni(II) Pb(I) Zn(II)

Figure 4.14 The solid phase color after extraction and detection of Hg(II) (0.025μM) and various metal ions (2.5 μM).

4.2.6 Method performance

Under suitable condition, the concentration range for Hg(II) detection by naked eyes was between 2 to 100 μg/L as shown in color stripe in Figure 4.15. Then, the accuracy of this method was evaluated by analyzing solution and water samples (drinking water, tap water) spiked with 10 μg/L Hg(II) ions. The solid phases obtained after extraction and reduction of Hg(II) from these three spiked samples show nearly the same distinct color indicating that the matrix in water did not affect Hg(II) detection. In the addition, when compared the sample phase to the standard phase color stripe, the concentration of Hg(II) in samples spiked with 10 μg/L Hg(II) ions was observed to be between 5 and 20 μg/L. The method has acceptable accuracy in the semi-quantitative analysis of Hg(II) in water samples.
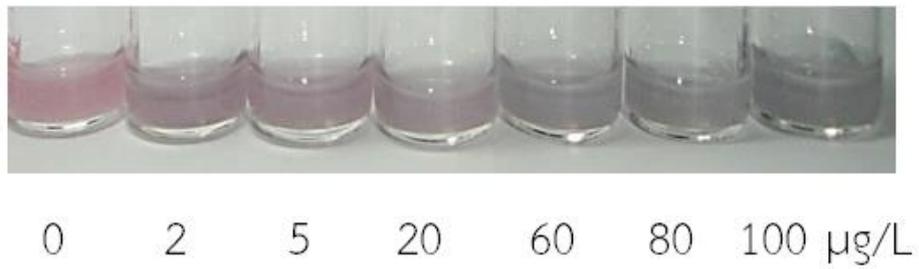
Figure 4.15 The standard solid color stripe and solid phase color in water sample analysis.

CHAPTER V

CONCLUSIONS

In this research, the analysis method to analyze trace amount of Hg(II) ions using L-cysteine modified gold nanoparticles was investigated. The two systems both liquid and solid phases of L-cysteine modified gold nanoparticles was developed. In this study, the gold nanoparticles was prepared by using tri-sodium citrate as reducing agent.

5.1 Determination of Hg(II) ion by gold nanoparticles solution

The principle of our system is to use the aggregation of gold nanoparticles in the presence of Hg(II) ions. This phenomenon was monitored by measuring the red shift of λ_{max} of solutions. The change in the ratio of absorbance of gold nanoparticles at 670 nm to that of 520 nm ($A_{670/520}$) after the addition of Hg(II) ions into L-cysteine modified gold nanoparticles systems was monitored. The addition of L-cysteine resulting in the change in the $A_{670/520}$. After the addition of Hg(II) ions, the larger aggregation of cys-AuNPs resulting in the larger $A_{670/520}$ values depending on concentration of Hg(II) was obtained. First, the effects of modification time (1- 20 minutes) and NaCl concentration (0.01- 0.5 M) was optimized. The 10 minute modification time and 0.05 M NaCl were chosen to modify AuNPs surface with L-cysteine. Afterward, the detection time (1-20 minutes) and sample volume of 50, 100, 200 µL were studied. The 20 minutes of detection time and the 50 µL of sample were chosen for the determination step. Under the optimized condition, the effects of co-existing ions were investigated. Based on this study, our system was selective toward Hg(II) ions. The performance of developed method was evaluated. The good linearity of calibration curve (R^2=0.9894) was achieved for Hg(II) concentration ranging from 5 to 40 µg/L. Furthermore, the detection limit as low as 4.5 µg/L was obtained. However, this method was only applied for drinking water analysis, whereas it could not be applied to analyze the tap water sample. The method is required further development.

5.2 Determination of Hg(II) by L-cysteine modified AuNPs supported silica

In order to overcome the matric effect, this study was shifted into the new system, solid phase system. First, the AuNPs capping with CTAB was deposited on the silica particles. Then, L-cysteine was added to modify the AuNPs surface deposited on the silica particles to serve as the solid phase to trap Hg(II) ions. The adsorbed Hg(II) ions on the solid phase was directly reduced to Hg (0). Then, the color of solid phase was observed comparing with the cys-AuNP modified silica particles (blank) with bare eyes. The effects of gold nanoparticles concentration, coating time, L-cysteine concentration, extraction time, $SnCl_2$ concentration (reducing agent) and co-existing ions were investigated. The effects of concentration of AuNPs solution (0.1 to 0.5 mM) and coating time (5-30 minutes) was studied. The 0.5 mM AuNPs and 30 minute coating time were chosen to coat AuNPs on solid phase. Then, the optimized L-cysteine concentration for modifying the AuNPs on solid phase was found to be 10 mM. Last, the extraction time of 5-30 minutes and $SnCl_2$ concentration ranging from 0.001 to 0.1 M were optimized. The optimized extraction time was 30 minutes where 0.01M $SnCl_2$ was chosen to reduce Hg(II) ions for analysis. Under the optimized condition, the effect of co-existing ions was investigated which the co-existing ions did not interfere for this analysis. Then, the developed method showed the excellent selectivity toward Hg(II) ions.

5.3 Suggestion of future work

- The sensitivity and selectivity of solution system should be developed to analyze of trace Hg(II) in sample water.

- The change of solid phase color should be improved to use in a wider range.

REFERENCES

1. Fan, A., et al., Direct colorimetric visualization of mercury (Hg^{2+}) based on the formation of gold nanoparticles. Talanta, 2010. 82(2): p. 687-692.

2. Miller, S., et al., Mercury-associated nephrotic syndrome: a case report and systematic review of the literature. Am J Kidney Dis, 2013. 62(1): p. 135-138.

3. Rodriguez, O., et al., Concerns on liquid mercury and mercury-containing wastes: a review of the treatment technologies for the safe storage. J Environ Manage, 2012. 101: p. 197-205.

4. Martin-Yerga, D., M.B. Gonzalez-Garcia, and A. Costa-Garcia, Electrochemical determination of mercury: a review. Talanta, 2013. 116: p. 1091-1104.

5. Chen, J., et al., Target-induced formation of gold amalgamation on DNA-based sensing platform for electrochemical monitoring of mercury ion coupling with cycling signal amplification strategy. Anal Chim Acta, 2014. 810: p. 10-16.

6. Ding, L., et al., Polystyrenesulfonate doped poly(Hydroxymethyl 3,4-Ethylenedioxythiophene) stabilized Au nanoparticle modified glassy carbon electrode as a reusable sensor for mercury(II) detection in chloride media. Journal of Electroanalytical Chemistry, 2013. 704: p. 96-101.

7. Puanngam, M., P.K. Dasgupta, and F. Unob, Automated on-line preconcentration of trace aqueous mercury with gold trap focusing for cold vapor atomic absorption spectrometry. Talanta, 2012. 99: p. 1040-1045.

8. Yuan, X., et al., An effective analytical system based on a pulsed direct current microplasma source for ultra-trace mercury determination using gold amalgamation cold vapor atomic emission spectrometry. Spectrochimica Acta Part B: Atomic Spectroscopy, 2014. 93: p. 1-7.

9. Qin, D., et al., Ultraviolet vapor generation atomic fluorescence spectrometric determination of mercury in natural water with enrichment by on-line solid phase extraction. Spectrochimica Acta Part B: Atomic Spectroscopy, 2013. 88: p. 10-14.

10. Zhang, W.B., et al., Evaluation of a new electrolytic cold vapor generation system for mercury determination by AFS. Talanta, 2010. 80(5): p. 2106-2112.

11. Chai, X., et al., Solid phase extraction of trace Hg(II) on silica gel modified with 2-(2-oxoethyl)hydrazine carbothioamide and determination by ICP-AES. Talanta, 2010. 82(5): p. 1791-1796.

12. Pontes, F.V.M., et al., Investigation of the Grignard reaction and experimental conditions for the determination of inorganic mercury and methylmercury in crude oils by GC–ICP-MS. Fuel, 2014. 116: p. 421-426.

13. Zhu, X. and S.D. Alexandratos, Determination of trace levels of mercury in aqueous solutions by inductively coupled plasma atomic emission spectrometry: Elimination of the 'memory effect'. Microchemical Journal, 2007. 86(1): p. 37-41.

14. Gao, Y., et al., Direct determination of mercury in cosmetic samples by isotope dilution inductively coupled plasma mass spectrometry after dissolution with formic acid. Anal Chim Acta, 2014. 812: p. 6-11.

15. Rodrigues, J.L., et al., Methylmercury and inorganic mercury determination in blood by using liquid chromatography with inductively coupled plasma mass spectrometry and a fast sample preparation procedure. Talanta, 2010. 80(3): p. 1158-1163.

16. Vilela, D., M.C. Gonzalez, and A. Escarpa, Sensing colorimetric approaches based on gold and silver nanoparticles aggregation: chemical creativity behind the assay. A review. Anal Chim Acta, 2012. 751: p. 24-43.

17. Bi, N., et al., Spectrophotometric determination of mercury(II) ion using gold nanorod as probe. Sensors and Actuators B: Chemical, 2012. 166-167: p. 766-771.

18. Liang, X., et al., Colorimetric detection of melamine in complex matrices based on cysteamine-modified gold nanoparticles. Analyst, 2011. 136(1): p. 179-183.

19. Xiao, Q., et al., Gold nanoparticle-based optical probes for sensing aminothiols. TrAC Trends in Analytical Chemistry, 2012. 40: p. 64-76.

20. Xiao, Q., L. Zhang, and C. Lu, Resonance light scattering technique for simultaneous determination of cysteine and homocysteine using fluorosurfactant-capped gold nanoparticles. Sensors and Actuators B: Chemical, 2012. 166-167: p. 650-657.

21. Bansal, N., et al., Determination of total mercury in bauxite and bauxite residue by flow injection cold vapour atomic absorption spectrometry. Microchemical Journal, 2014. 113: p. 36-41.

22. Lemos, V.A. and L.O. dos Santos, A new method for preconcentration and determination of mercury in fish, shellfish and saliva by cold vapour atomic absorption spectrometry. Food Chem, 2014. 149: p. 203-207.

23. Pietilä, H., et al., Determination of methyl mercury in humic-rich natural water samples using N2-distillation with isotope dilution and on-line purge and trap GC-ICP-MS. Microchemical Journal, 2014. 112: p. 113-118.

24. Anbazhagan, V., K.B.A. Ahmed, and S. Janani, Synthesis of catalytically active silver nanoparticles using lipid derived signaling molecule, N-steroylethanolamine: Promising antibacterial agent and selective colorimetric sensor for mercury ion. Sensors and Actuators B: Chemical, 2014. 200: p. 92-100.

25. Wang, G.L., et al., Ultrasensitive and dual functional colorimetric sensors for mercury (II) ions and hydrogen peroxide based on catalytic reduction property of silver nanoparticles. Biosens Bioelectron, 2012. 31(1): p. 337-342.

26. Jin, L.-H. and C.-S. Han, Eco-friendly colorimetric detection of mercury(II) ions using label-free anisotropic nanogolds in ascorbic acid solution. Sensors and Actuators B: Chemical, 2014. 195: p. 239-245.

27. Maity, D., et al., Colorimetric detection of mercury(II) in aqueous media with high selectivity using calixarene functionalized gold nanoparticles. Colloids and Surfaces A: Physicochemical and Engineering Aspects, 2014. 455: p. 122-128.

28. Basu, S., et al., Biomolecule induced nanoparticle aggregation: effect of particle size on interparticle coupling. J Colloid Interface Sci, 2007. 313(2): p. 724-734.

29. Hammond, J., et al., Localized Surface Plasmon Resonance as a Biosensing Platform for Developing Countries. Biosensors, 2014. 4(2): p. 172-188.

30. Liu, Z., et al., Resonance scattering amplification assay of biomolecules based on the biomineralization of gold nanoparticles bioconjugates. J Colloid Interface Sci, 2011. 363(1): p. 182-186.

31. Khan, M.S., G.D. Vishakante, and H. Siddaramaiah, Gold nanoparticles: a paradigm shift in biomedical applications. Adv Colloid Interface Sci, 2013. 199-200: p. 44-58.

32. Ah, C.S., et al., Colorimetric quantitative sensing of alkali metal ions based on reversible assembly and disassembly of gold nanoparticles. Current Applied Physics, 2013. 13(9): p. 1889-1893.

33. Krishnamurthy, S. and Y.-S. Yun, Recovery of microbially synthesized gold nanoparticles using sodium citrate and detergents. Chemical Engineering Journal, 2013. 214: p. 253-261.

34. Sener, G., L. Uzun, and A. Denizli, Lysine-promoted colorimetric response of gold nanoparticles: a simple assay for ultrasensitive mercury(II) detection. Anal Chem, 2014. 86(1): p. 514-520.

35. Lin, J., W. Zhou, and C.J. O'Connor, Formation of ordered arrays of gold nanoparticles from CTAB reverse micelles. Materials Letters, 2001. 49(5): p. 282-286.

36. Moon, S.Y., T. Kusunose, and T. Sekino, CTAB-Assisted Synthesis of Size- and Shape-Controlled Gold Nanoparticles in SDS Aqueous Solution. Materials Letters, 2009. 63(23): p. 2038-2040.

37. Wang, J., et al., Rapid and selective detection of cysteine based on its induced aggregates of cetyltrimethylammonium bromide capped gold nanoparticles. Anal Chim Acta, 2008. 626(1): p. 37-43.

38. Nishi, H. and S. Kobatake, Facile preparation of gold nanoparticle with diarylethene polymers by disodium malate and its photoreversible optical properties. Dyes and Pigments, 2012. 92(2): p. 847-853.

39. Khan, Z., et al., Au(III)-CTAB reduction by ascorbic acid: preparation and characterization of gold nanoparticles. Colloids Surf B Biointerfaces, 2013. 104: p. 11-17.

40. Kumar, S.G., K. S. and Kumar, R., Modeling of Formation of Gold Nanoparticles by Citrate Method. Ind. Eng. Chem. Res., 2007. 46 p. 3128-3136.

41. Abate, Y., et al., Nanometer-scale size dependent imaging of cetyl trimethyl ammonium bromide (CTAB) capped and uncapped gold nanoparticles by apertureless near-field optical microscopy. Chemical Physics Letters, 2009. 474(1-3): p. 146-152.

42. Wu, J., et al., Colorimetric assay for mercury (II) based on mercury-specific deoxyribonucleic acid-functionalized gold nanoparticles. Anal Chim Acta, 2011. 694(1-2): p. 115-119.

43. Chansuvarn, W. and A. Imyim, Visual and colorimetric detection of mercury(II) ion using gold nanoparticles stabilized with a dithia-diaza ligand. Microchimica Acta, 2011. 176(1-2): p. 57-64.

44. Ding, N., et al., A simple colorimetric sensor based on anti-aggregation of gold nanoparticles for Hg2+ detection. Colloids and Surfaces A: Physicochemical and Engineering Aspects, 2012. 395: p. 161-167.

45. Karthika, C.a.S., M., Removal of Hg (II) ions from aqueous solution by Acid Acrylic Resin.pdf. Environment Sciences, 2012. 1(1): p. 34-41.

46. Song, B.Y., Y. Eom, and T.G. Lee, Removal and recovery of mercury from aqueous solution using magnetic silica nanocomposites. Applied Surface Science, 2011. 257(10): p. 4754-4759.

47. Bagheri, H. and A. Gholami, Determination of very low levels of dissolved mercury(II) and methylmercury in river waters by continuous flow with on-line UV decomposition and cold-vapor atomic fluorescence spectrometry after pre-concentration on a silica gel-2-mercaptobenzimidazol sorbent. Talanta, 2001. 55(6): p. 1141-1150.

48. Delacote, C., et al., Factors affecting the reactivity of thiol-functionalized mesoporous silica adsorbents toward mercury(II). Talanta, 2009 . 79(3): p. 877-886.

APPENDIX

VITA

Miss Viphavee Liangraksa was born on July 10, 1986 in Lopburi, Thailand. She received a Bachelor of Science in chemistry from Srinakarinwirot University in 2007. She received a Graduate Diploma Program in Teaching Profession from Srinakarinwirot in 2008. Since 2011, she has been a graduate student at the Department of Chemistry, Faculty of Science, Chulalongkorn University and become a member of Environmental Analysis Research Unit (EARU) under supervision of Assistant Professor Dr. Fuangfa Unob, advisor, and Dr.Luxana Dubas, co-advisor. She completed her Master of Science in analytical chemistry in 2013.